# Electronic Supplementary Information (ESI)

## Highly sensitive and selective fluorescent sensor for copper(II) based on salicylaldehyde schiff-base derivatives with aggregation induced emission and mechanoluminescence

**Xiaoli Yang, Wenyan Zhang, Zihan Yi, Hao Xu, Jun Wei, Lingyun Hao[1]**

***College of Material Engineering, Jinling Institute of Technology, Nanjing 211169, P. R. China***

**New Journal of Chemistry**

*Corresponding author. Phone: +86-25-86188617. Fax: +86-25-86188617.

E-mail: haoly@jit.edu.cn

Corresponding author.
E-mail address: haoly@jit.edu.cn.

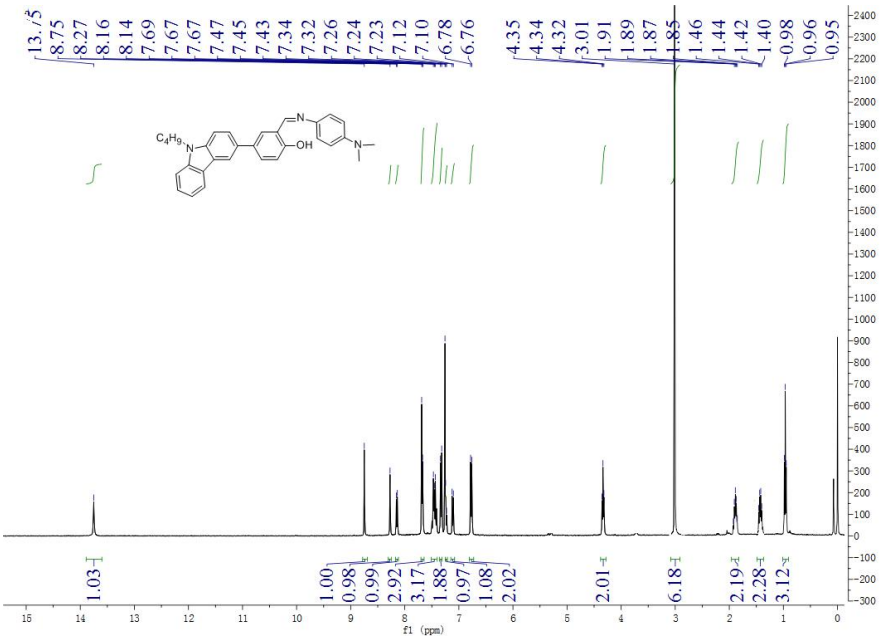
13.75
8.75
8.27
8.16
8.14
7.69
7.67
7.67
7.47
7.45
7.43
7.34
7.32
7.26
7.24
7.23
7.12
7.10
6.78
6.76
4.35
4.34
4.32
3.01
1.91
1.89
1.87
1.85
1.46
1.44
1.42
1.40
0.98
0.96
0.95
1.03
1.00
0.98
0.99
2.92
3.17
1.88
0.97
1.08
2.02
2.01
6.18
2.19
2.28
3.12
f1 (ppm)

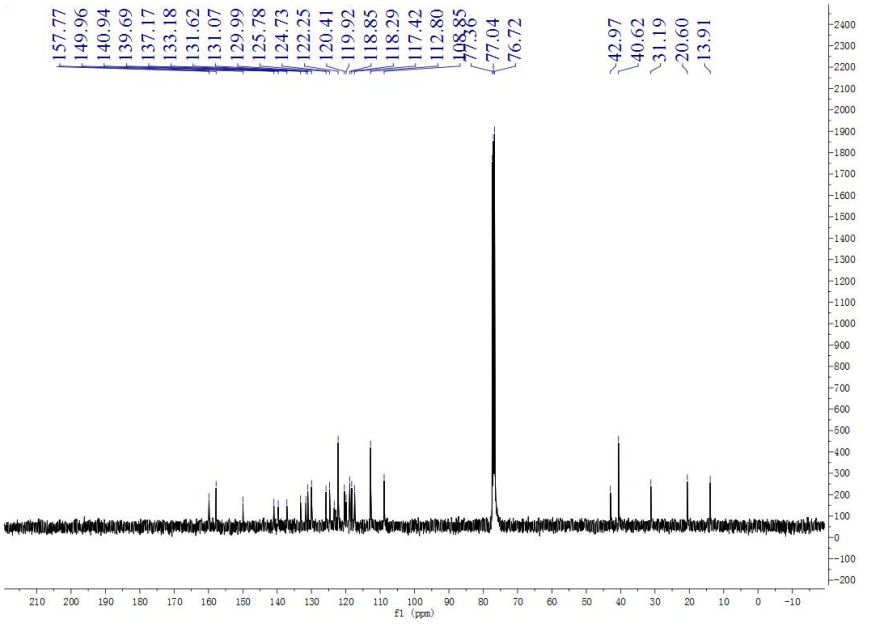
157.77
149.96
140.94
139.69
137.17
133.18
131.62
131.07
129.99
125.78
124.73
122.25
120.41
119.92
118.85
118.29
117.42
112.80
108.85
77.36
77.04
76.72
42.97
40.62
31.19
20.60
13.91
f1 (ppm)

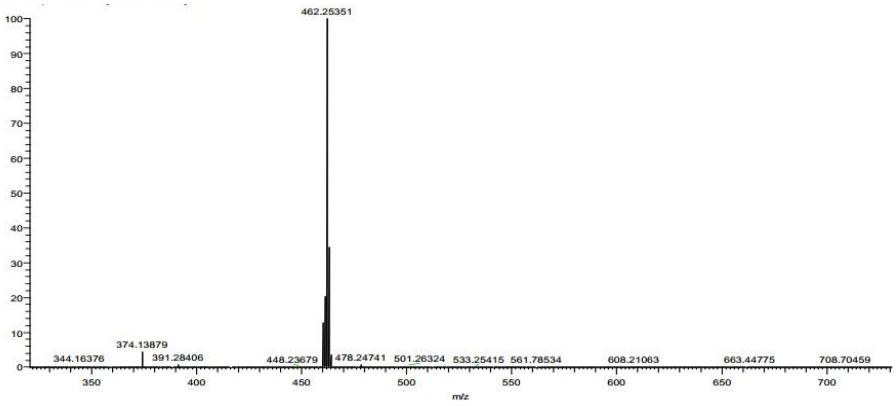


Figure S1. $^{1}H$ NMR , $^{13}C$ NMR and MS spectra of **A1.**

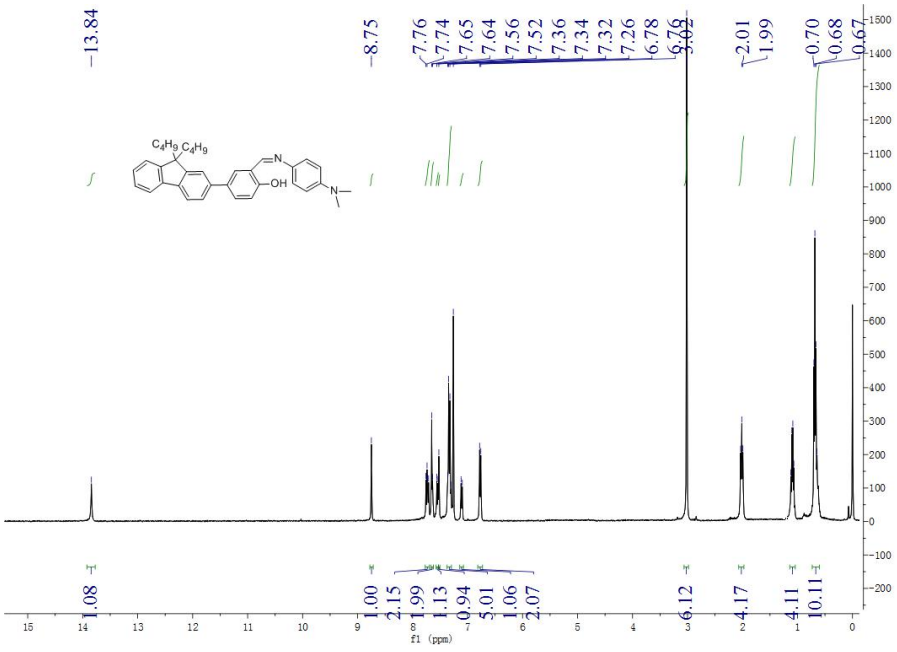

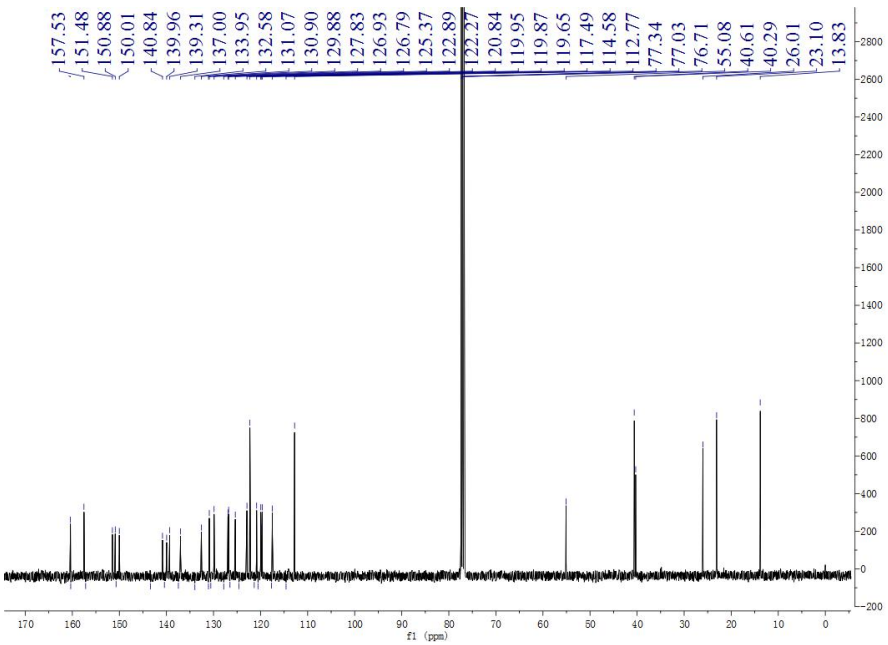


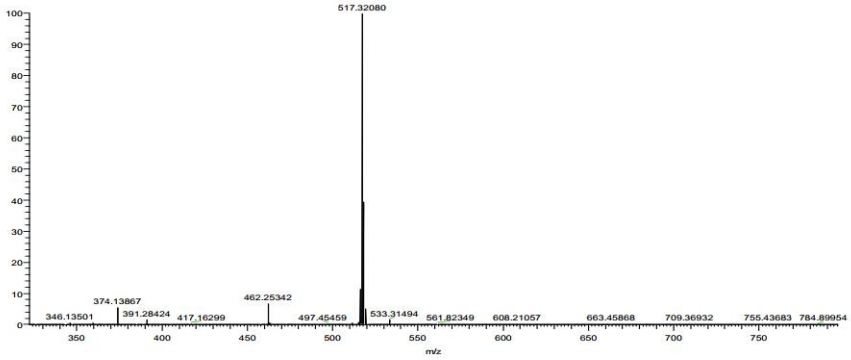


Figure S2. $^{1}H$ NMR , $^{13}C$ NMR and MS spectra of **A2.**

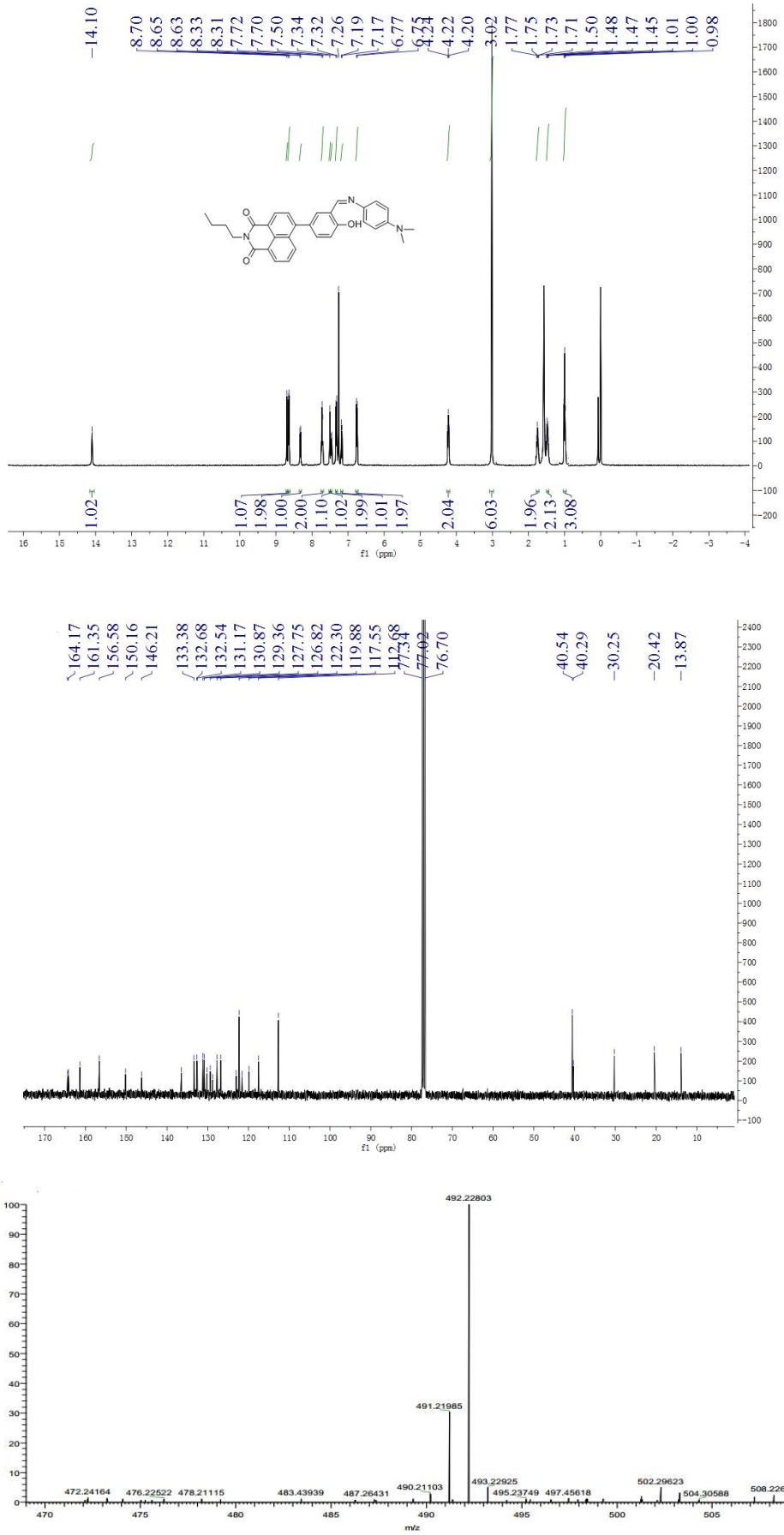


Figure S3. $^{1}H$ NMR , $^{13}C$ NMR and MS spectra of **A3.**

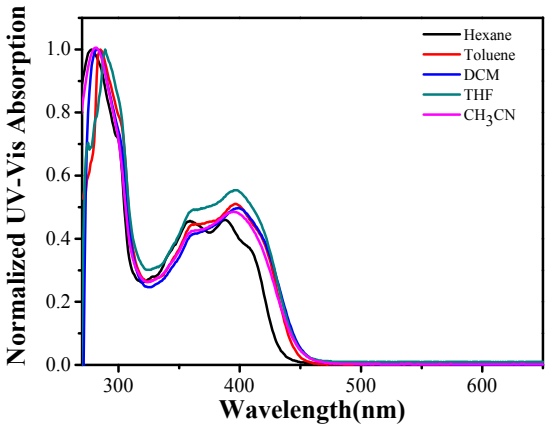


Figure S4. Normalized UV–vis absorption spectra of **A1** in different solvents.

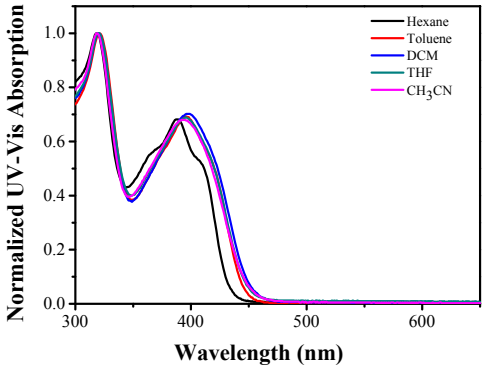


Figure S5. Normalized UV–vis absorption spectra of **A2** in different solvents.

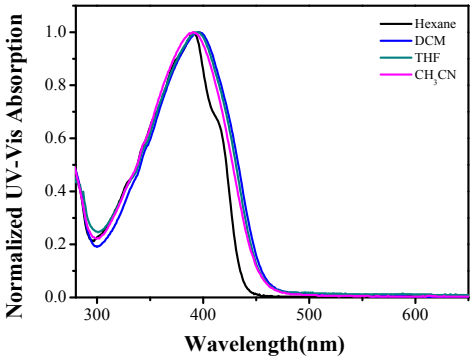


Figure S6. Normalized UV–vis absorption spectra of **A3** in different solvents.

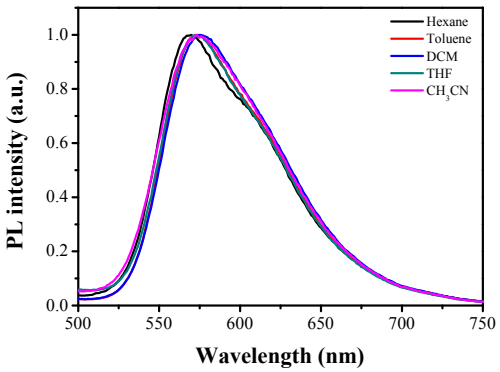


Figure S7. Normalized emission spectra of **A2** in different solvents.

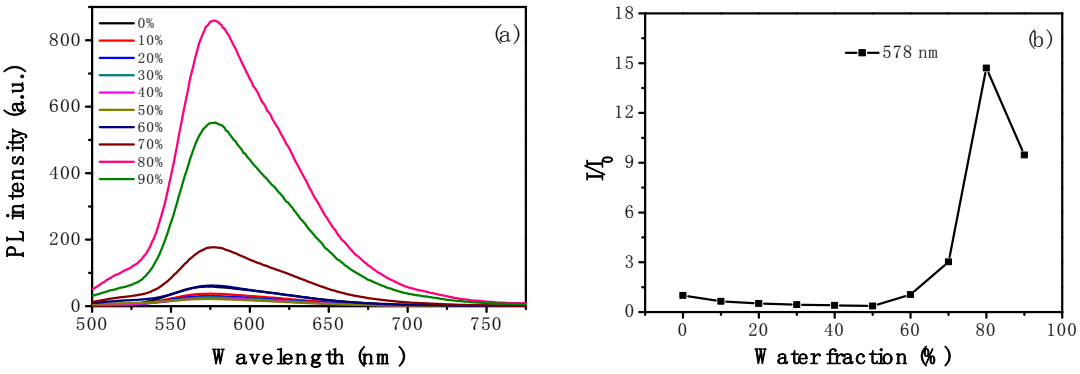


Figure S8. (a) The fluorescence spectra of **A2** in $CH_3CN$–$H_2O$ with different $H_2O$ fractions (vol., 0–90%). (b) Plot of $I/I_0$ vs. water content of the solvent mixture, where $I_0$ is the PL intensity in pure $CH_3CN$ solution of **A2** in $CH_3CN$–water under irradiation of UV lamp at 365 nm.

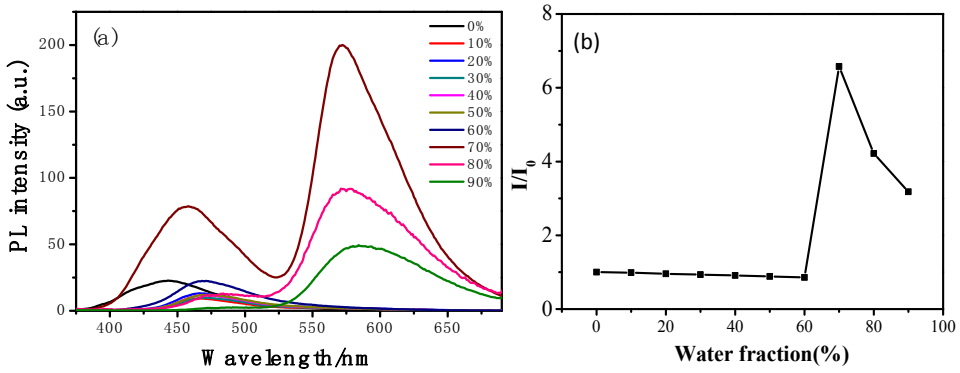


Figure S9. (a) The fluorescence spectra of **A3** in $CH_3CN$–water with different water fractions (vol., 0–90%). (b) Plot of $I/I_0$ vs. water content of the solvent mixture, where $I_0$ is the PL intensity in pure $CH_3CN$ solution of **A3** in $CH_3CN$–water under irradiation of UV lamp at 365 nm.

**Table S1.** Crystallographic data of **A3** (CCDC 1557524)

| | **A3** |
|---|---|
| formula | $C_{31}$ $H_{29}N_3$ $O_3$ |
| fw | 491.57 |
| crystal system | Triclinic |
| space group | P-1 (2) |
| *a*, Å | 7.6919(13) |
| *b*, Å | 8.8249(14) |
| *c*, Å | 19.317(4) |
| *a*, deg | 78.851(5) |
| *β*, deg | 85.259(6) |
| γ, deg | 82.477(5) |
| *V*, Å$^3$ | 1273.2(4) |
| *Z* | 2 |
| $\rho_{calcd}$,g cm$^{-3}$ | 1.28215 |
| *T* / K | 296(2) |
| $\mu$, mm$^{-1}$ | 1.282 |
| $\theta$, deg | 2.37 to 27.41 |
| *F*(000) | 520 |
| index ranges | –9 ≤ h ≤ 6, –10 ≤ k ≤ 1-, –22 ≤ l ≤ 22 |
| data/restraints/parameters | 4454/ 0 / 338 |
| GOF ($F^2$) | 0.982 |
| $R_1^a$,$wR_2^b$ (I>2σ(I)) | 0.0585, 0.1296 |
| $R_1^a$, $wR_2^b$ (all data) | 0.1111,0.0537 |

$R_1^a = \Sigma||F_o| - |F_c||/\Sigma F_o|$. $wR_2^b = [\Sigma w(F_o^2 - F_c^2)^2/\Sigma w(F_o^2)^2]^1$

**Table S2.** Summary of the molecular interactions in the crystal

| Bond distances (Å) | | | |
|---|---|---|---|
| C(9)-N(3) | 1.28(30) | C(15)-O(1) | 1.35(30) |
| C(9)-C(10) | 1.46(36) | N(3)-C(6) | 1.42(34) |
| C(10)-C(15) | 1.41(39) | C(12)-C(16) | 1.49(31) |
| C(27)-O(3) | 1.22(33) | C(3)-N(2) | 1.37 (37) |

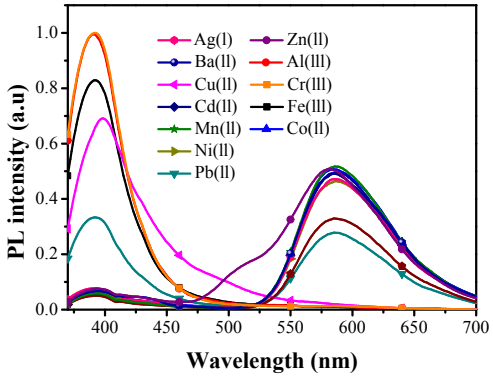


Figure S10. Fluorescence spectra of **A1** upon adding of 10 equiv. different nitrate salts in water solution($1.0\times10^{-5}$ M, $CH_3CN$ )

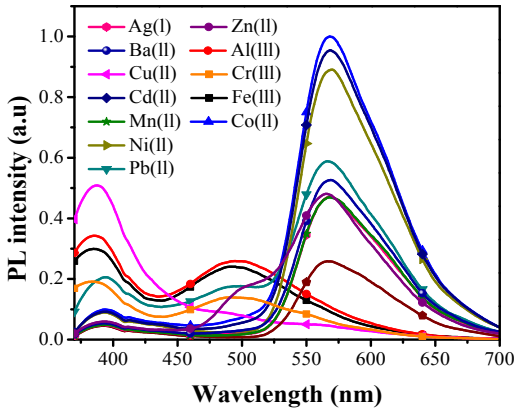


Figure S11. Fluorescence spectra of **A2** upon adding of 10 equiv. different nitrate salts in water solution($1.0\times10^{-5}$ M, $CH_3CN$ )

**Table S3**. Comparison of some Schiff base chemosensors for $Cu^{2+}$ detection

| NO | Structure of sensors | Detection limit (μM) | Linear range (μM) | Quantum yield | Interference | References |
|---|---|---|---|---|---|---|
| 1 | 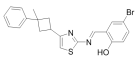 | 0.0088 | 0.01-570 | No data | None | 13 |
| 2 | 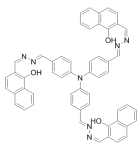 | 10.64 *$10^{-3}$ | 0.2-0.8 | No data | None | 14 |
| 3 | 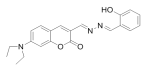 | 0.27 | 0-10 | 11.5%. | None | 15 |
| 4 | 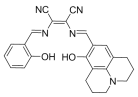 | 7.3 | 0-80 | No data | None | 16 |
| 5 | 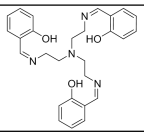 | 1.5 | 0-20 | No data | $Fe^{2+}$ and $Zn^{2+}$ | 18 |
| 6 | 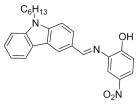 | 3.62 | 6-20 | No data | $Fe^{3+}$ | 19 |
| 7 | 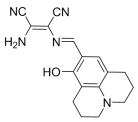 | 2.1 | 0.10-10.00 | No data | None | 20 |
| 8 | 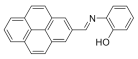 | 0.97 | 0-50 | 28.4% | None | 28 |
| 9 | 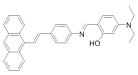 | 0.212 | 0-7.5 | 29.5% | None | 29 |
| 10 | 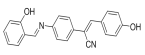 | 1.5 | 0-10 | 1.5% | None | 30 |
| 11 | 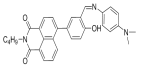 | 0.23 | 0-20 | 7.5% | None | This work |

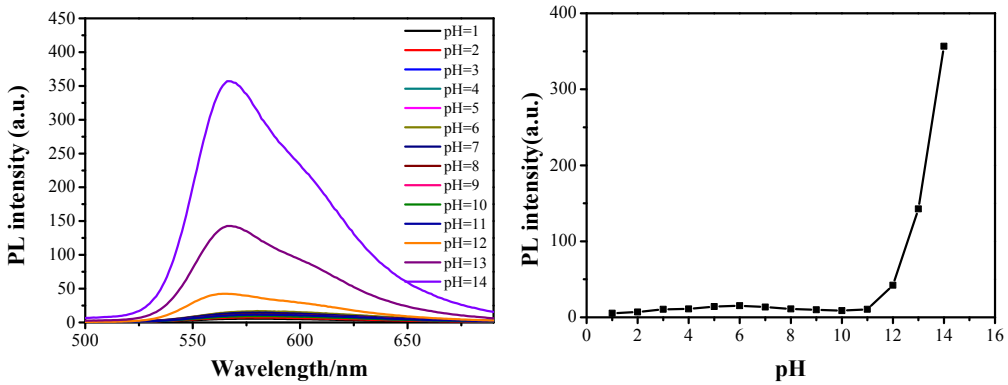


Figure S12. (a) pH-dependence of the emission spectra of **A3** in $CH_3CN$-buffer mixture with volume ratio 1:9; (b) change in the PL intensity with varying the pH range (1-14) at maximum PL intensity.